A&A 405, 779–786 (2003)
DOI: 10.1051/0004-6361:20030664

Astronomy & Astrophysics

Time-dependent coupling of solar oscillations

M. Roth⋆ and M. Stix

Kiepenheuer-Institut für Sonnenphysik, Schöneckstr. 6, 79104 Freiburg, Germany

Received 18 October 2002 / Accepted 5 May 2003

Abstract. We investigate the effects of a large-scale time-dependent flow in the solar convection zone on the solar *p*-mode oscillations. The theory of time-dependent perturbations is applied, and we concentrate on flow fields that can be described by a single harmonic in space and time. An iterative method of obtaining approximate analytical solutions to the equations of the coupled oscillator is outlined. Example calculations are presented for the special case of two coupling partners. Special attention is paid to the resonance that occurs when the time dependence of the flow meets the beat frequency of two *p* modes. We conclude that time-dependent flow fields in the solar convection zone may diminish the height of the peaks in the oscillation power spectrum, and may contribute to their asymmetry, broadening, and effective shift.

Key words. Sun: convection – Sun: oscillations

1. Introduction

The interaction of the large-scale velocity field on the Sun with the global solar oscillations is best known from the rotationally induced splitting of *p*-mode frequencies into multiplets. Typically this splitting occurs for a toroidal velocity field such as rotation, and results from *self-coupling* of individual eigenoscillations. In contrast to this, a poloidal velocity field may couple two different oscillations, especially when their frequencies lie close together, which is called *quasi-degeneracy*. Lavely & Ritzwoller (1992) have outlined the application of perturbation theory to quasi-degenerate oscillations, and Roth & Stix (1999) have calculated the effect of a steady-state poloidal velocity upon the oscillation frequencies. This theory has been used to derive upper limits for large-scale poloidal velocity fields in the solar convection zone (Roth et al. 2002).

On the other hand, the velocity field in the solar convection zone is not steady. Especially the small-scale flow, e.g. the granulation, is strongly variable, on time scales of minutes. Larger-scale flow components have longer lifetimes, e.g. up to several days for the supergranulation, and weeks to months for velocity fields that have a scale comparable to the depth of the convection zone. Thus, since the coupling velocity varies with time, its effects on the solar oscillations must be time-dependent, too. We have pointed out earlier (Roth & Stix 2001) that a time-dependent perturbation may lead to a transfer of oscillation energy between the modes that participate in the coupling. In the present paper we shall further study this subject. But we shall restrict the case to large-scale motions that vary slowly in comparison with the oscillations themselves. Moreover, in spite of the time-dependence of the velocity field $\boldsymbol{v}_0$, we use the condition

$$\nabla \cdot (\rho_0 \boldsymbol{v}_0) = 0\,, \tag{1}$$

which characterizes *anelastic* variations, where the density variation related to $\boldsymbol{v}_0$ is neglected.

The coupling of solar *p*-mode oscillations has a well-known analogy in the coupling of pendulums. Let two uncoupled pendulums with masses m_1 and m_2 oscillate with frequencies ω_1 and ω_2, respectively. Coupling with a spring constant k yields an equation

$$m_1(\ddot{x}_1 + \omega_1^2 x) + k(x_1 - x_2) = 0 \tag{2}$$

for the amplitude $x_1(t)$ of the first pendulum, and a corresponding equation for $x_2(t)$, with the subscripts 1 and 2 exchanged. If k is constant, the system oscillates with two frequencies,

$$\omega_\pm^2 = \frac{\omega_1^2+\omega_2^2}{2} + \frac{k}{2}\left(\frac{1}{m_1}+\frac{1}{m_2}\right) \pm \frac{1}{2}\sqrt{k^2\left(\frac{1}{m_1}+\frac{1}{m_2}\right)^2 + 2k\left(\frac{1}{m_1}-\frac{1}{m_2}\right)\left(\omega_1^2-\omega_2^2\right) + \left(\omega_1^2-\omega_2^2\right)^2}\,. \tag{3}$$

If the coupling is weak (small k), the new frequencies lie in the vicinity of ω_1 and ω_2. Such is also the case for the coupling of solar *p* modes by a stationary large-scale flow (Roth & Stix 1999). We shall see below that, when the coupling is time-dependent, additional frequencies appear. These additional frequencies reflect the time dependence of the flow; they also lie in the vicinity of the original frequencies if the flow variation is slow.

Send offprint requests to: M. Roth,
e-mail: mroth@kis.uni-freiburg.de

⋆ *Present address:* Freiburg Center for Data Analysis and Modelling, Eckerstr. 1, 79104 Freiburg, Germany.

In the subsequent two sections we shall outline the theory for time-dependent perturbations and describe an iterative method of solution. In Sect. 4, then, we apply the general scheme to the special case of two coupling solar p modes, and discuss the possible effects on the appearance of such modes in the power spectrum.

2. Time-dependent perturbation theory

The starting point is the unperturbed equation of oscillation,

$$H_0(\boldsymbol{r})\boldsymbol{\xi}_n(\boldsymbol{r},t) = -\rho_0\omega_n^2\boldsymbol{\xi}_n(\boldsymbol{r},t), \tag{4}$$

where the operator $H_0(\boldsymbol{r})$ contains the diverse force terms like pressure gradient, etc., all written as linear expressions in terms of the oscillation vector $\boldsymbol{\xi}(\boldsymbol{r},t)$, see, e.g., Stix (2002). We consider the complete set of solutions $\boldsymbol{\xi}_n(\boldsymbol{r},t)$ as known; the index n represents the triple of quantum numbers – radial order, harmonic degree, and azimuthal order. We seek solutions that are influenced by a time-dependent perturbation and which therefore satisfy the equation

$$[H_0(\boldsymbol{r}) + \varepsilon H_1(\boldsymbol{r},t)]\,\boldsymbol{\xi}(\boldsymbol{r},t) = \rho_0\frac{\partial^2}{\partial t^2}\boldsymbol{\xi}(\boldsymbol{r},t), \tag{5}$$

where the perturbation operator is $\varepsilon H_1(\boldsymbol{r},t) = -2\rho_0\boldsymbol{v}_0\cdot\nabla\partial/\partial t$, and the large-scale velocity $\boldsymbol{v}_0$ is poloidal, and proportional to a single harmonic of degree s and azimuthal order t. Its radial component is defined by

$$u_s^t(r,t) = u_{\max}\frac{4(r_\odot - r)(r - r_{\rm conv})}{(r_\odot - r_{\rm conv})^2}\,\exp(\mathrm{i}\Omega t) \tag{6}$$

for $r_{\rm conv} \le r \le r_\odot$, and the other components follow from (1). The radii $r_{\rm conv}$ and $r_\odot$ mark the lower and upper boundaries of the convection zone. Expression (6) is an elementary form of a large-scale flow; this flow varies harmonically between two maximal values and changes the direction in between. For the frequency of this variation we require $|\Omega| \ll |\omega_n|$, where ω_n is any of the involved eigenfrequencies. Other forms may be composed of a sum of terms of this type.

We expand the general solution $\boldsymbol{\xi}(\boldsymbol{r},t)$ in terms of the set $\boldsymbol{\xi}_n$,

$$\boldsymbol{\xi}(\boldsymbol{r},t) = \sum_n c_n(t)\boldsymbol{\xi}_n(\boldsymbol{r})\mathrm{e}^{-\mathrm{i}\omega_n t}. \tag{7}$$

Here, the time-dependence that is connected to $\boldsymbol{\xi}_n$ is explicitly given, and the same symbol, $\boldsymbol{\xi}_n$, is used for the time-independent part. In the case $H_1(\boldsymbol{r},t) \equiv 0$ the expansion coefficients $c_n(t)$ are constants determined by the initial excitation of the oscillations $\boldsymbol{\xi}_n$. Otherwise and in contrast to the perturbation theory for a stationary operator $H_1(\boldsymbol{r})$, the expansion coefficients c_n are now time-dependent. The coefficients $c_n(t)$ obey a set of equations which are obtained by substituting (7) into Eq. (5),

$$\rho_0\sum_n(\ddot{c}_n - 2\mathrm{i}\omega_n\dot{c}_n)\boldsymbol{\xi}_n\exp(-\mathrm{i}\omega_n t) = \varepsilon\sum_n c_n H_1(\boldsymbol{r},t)\boldsymbol{\xi}_n\exp(-\mathrm{i}\omega_n t), \tag{8}$$

where we have used Eq. (4). An equation for $c_m(t)$ is now obtained by scalar multiplication by $\boldsymbol{\xi}_m^*(\boldsymbol{r})$, integration over the whole volume of the Sun, and use of the orthogonality of the oscillation eigenfunctions,

$$\int\rho_0\boldsymbol{\xi}_{k'}^*\cdot\boldsymbol{\xi}_k\,\mathrm{d}^3r = N_k\delta_{kk'}, \tag{9}$$

where

$$N_k = \int_0^{r_\odot}\rho_0\left[\xi_r\xi_r' + l(l+1)\xi_h\xi_h'\right]r^2\,\mathrm{d}r, \tag{10}$$

and ξ_r and ξ_h define the radial and angular components of $\boldsymbol{\xi}$. Thus we find

$$\ddot{c}_m(t) - 2\mathrm{i}\omega_m\dot{c}_m(t) = \frac{\varepsilon}{N_m}\sum_n c_n(t)H_{mn}(t)\exp[\mathrm{i}(\omega_m - \omega_n)t]. \tag{11}$$

Here we have used the definition

$$H_{mn}(t) := \int\boldsymbol{\xi}_m^*\cdot H_1(\boldsymbol{r},t)\boldsymbol{\xi}_n\,\mathrm{d}^3r\,. \tag{12}$$

The matrix element H_{mn} vanishes in the case of poloidal velocity fields and self-coupling, $m = n$, as has been shown by Lavely & Ritzwoller (1992). This is different from the case of the coupled pendulums, where the term kx_1 in Eq. (2) leads to self-coupling.

The system (11) of ordinary differential equations is of second order with non-constant coefficients. It describes the evolution of the system of oscillations under the influence of the perturbation $H_1(\boldsymbol{r},t)$, and constitutes an initial-value problem by the specification of the coefficients at the instant $t = 0$, i.e., $c_m(0) = c_m^{(0)}$. There are various processes on the Sun that could be accounted for the perturbation $H_1(\boldsymbol{r},t)$. Here we shall concentrate on a time-dependent flow field in the convection zone.

The initial-value problem can be solved numerically for any configuration of the flow field. On the other hand, we may gather more insight into the system with the aid of approximate analytical solutions. A general analytical solution does not exist for an arbitrary time-dependence of H_1 (Walter 1993).

According to our choice (6) above we have

$$H_1(\boldsymbol{r},t) = H_1(\boldsymbol{r})\exp(\mathrm{i}\Omega t). \tag{13}$$

Hence the system (11) of differential equations takes the form

$$\ddot{c}_m - 2\mathrm{i}\omega_m\dot{c}_m = \frac{\varepsilon}{N_m}\sum_n c_n H_{mn}\mathrm{e}^{\mathrm{i}\Omega t}\mathrm{e}^{\mathrm{i}(\omega_m-\omega_n)t}. \tag{14}$$

Because of the time-dependence $\exp(\mathrm{i}\Omega t)$, the right-hand side is not Hermitian.

3. Iterative method

A closed analytical solution of the system (14) is not possible; but approximative methods can be used. One possibility to obtain an approximate solution is the ansatz

$$c_m(t) = c_m^{(0)}(t) + \varepsilon c_m^{(1)}(t) + \varepsilon^2 c_m^{(2)}(t) + \ldots \tag{15}$$

Substituting this into Eq. (14) we can sort in terms of powers of ε. Hence we can successively derive the time-dependent zero-order, first-order, ... contribution to the coefficient $c_m(t)$.

3.1. Zero order

Comparison of the coefficients that correspond to the zero-order in ε yields the differential equation

$$\ddot{c}_m^{(0)} - 2\mathrm{i}\omega_m \dot{c}_m^{(0)} = 0. \tag{16}$$

The solution of this equation is

$$c_m^{(0)} = A_m^{(0)} + B_m^{(0)} \mathrm{e}^{2\mathrm{i}\omega_m t} \tag{17}$$

with the constants of integration $A_m^{(0)}$ and $B_m^{(0)}$. As Eq. (7) holds for the eigenvector $\boldsymbol{\xi}(\boldsymbol{r}, t)$, we obtain the zero-order solution

$$\boldsymbol{\xi}^{(0)}(\boldsymbol{r}, t) = \sum_m \left(A_m^{(0)} \mathrm{e}^{-\mathrm{i}\omega_m t} + B_m^{(0)} \mathrm{e}^{\mathrm{i}\omega_m t} \right) \boldsymbol{\xi}_m(\boldsymbol{r}). \tag{18}$$

This means that the constants $A_m^{(0)}$ and $B_m^{(0)}$ belong to the two complex conjugate eigenoscillations.

3.2. First order

In the first order of the expansion (15) in powers of ε we find the equation

$$\ddot{c}_m^{(1)} - 2\mathrm{i}\omega_m \dot{c}_m^{(1)} = \frac{1}{N_m} \sum_n c_n^{(0)} H_{mn} \mathrm{e}^{\mathrm{i}\Omega t} \mathrm{e}^{\mathrm{i}(\omega_m - \omega_n)t}, \tag{19}$$

where we must substitute the coefficients $c_n^{(0)}$ given by (17). The differential Eq. (19) can be integrated easily by the method of the "variation of constants". We find

$$c_m^{(1)}(t) = \frac{1}{N_m} \sum_n H_{mn} \left[A_n^{(0)} \frac{\mathrm{e}^{\mathrm{i}(\Omega + \omega_m - \omega_n)t}}{\omega_m^2 - (\Omega - \omega_n)^2} + B_n^{(0)} \frac{\mathrm{e}^{\mathrm{i}(\Omega + \omega_m + \omega_n)t}}{\omega_m^2 - (\Omega + \omega_n)^2} \right]. \tag{20}$$

In general, a solution of form (17) must be added to this result, with constants that are specified by the initial conditions. For brevity, this contribution is not written down here.

3.3. Second order

The second order yields the differential equation

$$\ddot{c}_m^{(2)} - 2\mathrm{i}\omega_m \dot{c}_m^{(2)} = \frac{1}{N_m} \sum_n c_n^{(1)} H_{mn} \mathrm{e}^{\mathrm{i}\Omega t} \mathrm{e}^{\mathrm{i}(\omega_m - \omega_n)t}. \tag{21}$$

After substitution of the result (20) we find

$$\ddot{c}_m^{(2)} - 2\mathrm{i}\omega_m \dot{c}_m^{(2)} = \frac{1}{N_m} \sum_n H_{mn} \mathrm{e}^{\mathrm{i}\Omega t} \mathrm{e}^{\mathrm{i}(\omega_m - \omega_n)t} \times \left\{ \frac{1}{N_n} \sum_k H_{nk} \left[A_k^{(0)} \frac{\mathrm{e}^{\mathrm{i}(\Omega + \omega_n - \omega_k)t}}{\omega_n^2 - (\Omega - \omega_k)^2} + B_k^{(0)} \frac{\mathrm{e}^{\mathrm{i}(\Omega + \omega_n + \omega_k)t}}{\omega_n^2 - (\Omega + \omega_k)^2} \right] \right\}. \tag{22}$$

Integration yields the solution

$$c_m^{(2)}(t) = \frac{1}{N_m} \sum_n H_{mn} \frac{1}{N_n} \sum_k H_{nk} \times \left\{ A_k^{(0)} \frac{\mathrm{e}^{\mathrm{i}(2\Omega + \omega_m - \omega_k)t}}{[\omega_n^2 - (\omega_k - \Omega)^2]\,[\omega_m^2 - (\omega_k - 2\Omega)^2]} + B_k^{(0)} \frac{\mathrm{e}^{\mathrm{i}(2\Omega + \omega_m + \omega_k)t}}{[\omega_n^2 - (\Omega + \omega_k)^2]\,[\omega_m^2 - (2\Omega + \omega_k)^2]} \right\}. \tag{23}$$

Again a solution of form (17) must be added in order to be able to satisfy the initial conditions, in addition to terms arising from those parts of $c_m^{(1)}(t)$ that had been added to satisfy the initial conditions in the first order.

For higher orders we can continue in this manner. If the coupling is weak, i.e., if

$$\varepsilon |H_{mn}| \ll N_n \, |\omega_m^2 - \omega_n^2|, \tag{24}$$

the expansion will converge rapidly. The example given in the following section shows that good convergence can be obtained already from the first and second-order contributions.

A close view to the solutions (20) and (23) makes clear that in the diverse orders we obtain large contributions for eigenstates that are quasi-degenerate. In comparison to these, the contributions that result from oscillations with a large distance in frequency can be neglected.

The iterative method yields the next higher order from the preceding one by multiplication with $\exp[\mathrm{i}(\Omega + \omega_m - \omega_n)t]$ and subsequent integration. Because of this, ever higher harmonics of the fundamental frequencies Ω and $\omega_m - \omega_n$ appear, as well as combinations of these. Therefore the amplitude of the oscillation varies additionally with these harmonic "overtones".

4. The two-coupler system

In order to demonstrate the coupling of solar oscillations by a variable flow field, we now consider a system that consists only of two coupling modes.

4.1. Numerical and approximate solutions

In the case of two coupling modes we must solve the equations

$$\ddot{c}_1(t) - 2\mathrm{i}\omega_1 \dot{c}_1(t) = \frac{\varepsilon}{N_1} c_2(t) H_{12} \mathrm{e}^{\mathrm{i}\Omega t} \mathrm{e}^{\mathrm{i}(\omega_1 - \omega_2)t}, \tag{25}$$

$$\ddot{c}_2(t) - 2\mathrm{i}\omega_2 \dot{c}_2(t) = \frac{\varepsilon}{N_2} c_1(t) H_{21} \mathrm{e}^{\mathrm{i}\Omega t} \mathrm{e}^{\mathrm{i}(\omega_2 - \omega_1)t}. \tag{26}$$

We consider only the effect of a poloidal flow; therefore H_{12} and H_{21} are the only non-zero elements of the coupling matrix. The differential rotation, as a steady toroidal velocity, would only lead to frequency shifts and frequency splittings, but not to a variation of the oscillation amplitude. Hence it is not of interest for the present study.

The iterative method described above is based on the ansatz

$$\begin{aligned} c_1(t) &= c_1^{(0)}(t) + \varepsilon c_1^{(1)}(t) + \varepsilon^2 c_1^{(2)}(t) + \ldots, \\ c_2(t) &= c_2^{(0)}(t) + \varepsilon c_2^{(1)}(t) + \varepsilon^2 c_2^{(2)}(t) + \ldots, \end{aligned} \tag{27}$$

and yields the zero, first, and second-order contributions

$$c_1^{(0)}(t) = A_1^{(0)} + B_1^{(0)} \mathrm{e}^{2\mathrm{i}\omega_1 t}, \tag{28}$$

$$c_1^{(1)}(t) = \frac{H_{12}}{N_1} \left\{ A_2^{(0)} \frac{\mathrm{e}^{\mathrm{i}(\Omega + \omega_1 - \omega_2)t}}{\omega_1^2 - (\Omega - \omega_2)^2} + B_2^{(0)} \frac{\mathrm{e}^{\mathrm{i}(\Omega + \omega_1 + \omega_2)t}}{\omega_1^2 - (\Omega + \omega_2)^2} \right\}, \tag{29}$$

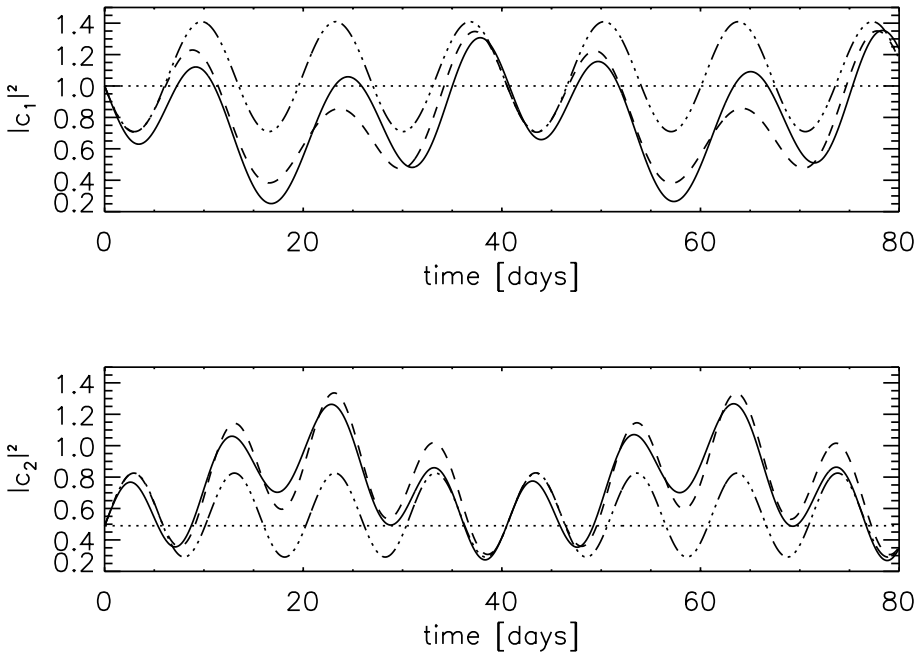

Fig. 1. Comparison of the numerical solution (solid line) of Eqs. (25) and (26) of the two-coupler system with the approximate solutions according to expansions (27), in zero (·····), first (– · · – · · –), and second (– – ––) order. The two modes have frequencies $\nu_1 = 3000\,\mu$Hz and $\nu_2 = 3001\,\mu$Hz. The initial conditions are $c_1(0) = 1$, $c_2(0) = 0.7$, and $\dot{c}_1(0) = \dot{c}_2(0) = 0$. The perturbation has the magnitude $\varepsilon|H_{12}|/\langle H_0\rangle = 0.02$ and a frequency $\Omega = 2\pi/(81$ days).

and

$$c_1^{(2)}(t) = \frac{H_{12}H_{21}}{N_1N_2}\left\{A_1^{(0)}\frac{\mathrm{e}^{2\mathrm{i}\Omega t}}{4\Omega(\Omega-\omega_1)[(\Omega-\omega_1)^2-\omega_2^2]}\right.$$
$$\left.+B_1^{(0)}\frac{\mathrm{e}^{2\mathrm{i}(\Omega+\omega_1)t}}{4\Omega(\Omega+\omega_1)[(\Omega+\omega_1)^2-\omega_2^2]}\right\}. \qquad (30)$$

As with the general scheme, solutions to the homogeneous part of (25) and (26) must be added in order to satisfy the initial conditions in all orders; the terms added for this purpose then create further contributions to the subsequent higher orders. The coefficient $c_2(t)$ is given by expressions analogous to (28)–(30), with the subscripts 1 and 2 interchanged.

For a special example we compare the approximate solutions with a numerical solution (Fig. 1). We take two oscillations with frequencies $\nu_1 = 3000\,\mu$Hz and $\nu_2 = 3001\,\mu$Hz, respectively, that are coupled by a time-dependent perturbation. This perturbation can be regarded as the real part of (6), with $\varepsilon|H_{12}|/\langle H_0\rangle = 0.02$ and $\Omega = 2\pi/(81$ days); $\langle H_0\rangle$ is defined by an integral of form (12). Initially the two oscillations have prescribed amplitudes, given by $c_1(0) = 1$, $\dot{c}_1(0) = 0$, and $c_2(0) = 0.7$, $\dot{c}_2(0) = 0$. For the perturbation we use the initial condition $H_1(r, 0) = 0$.

If there was no coupling, the coefficients c_1 and c_2 would keep their initial values. In fact this state is represented by the zero-order approximate solution. The approximate solutions of higher orders, as well as the numerical solution, show the variation of c_1 and c_2 around those initial values. Figure 1 demonstrates that the numerical solution is rather well approximated in the second order already.

At first sight it would appear that the first and second-order solutions, as well as the numerical solution, fail to satisfy the initial conditions $\dot{c}_i(0) = 0$. Actually they do so by means of contributions that vary on the fast time scale $1/\omega_i$ of the two p modes, and that have amplitudes of magnitude $|\Omega/\omega_i|$ or $|(\omega_2 - \omega_1)/\omega_i|$ relative to the amplitudes of the leading terms. The scales of Fig. 1 are such that these contributions are suppressed.

The example shows that time-dependent coupling of solar oscillations can cause large variations of the amplitude of the diverse modes. Moreover, the approximate solution makes clear that these variations are superpositions of oscillations with certain frequencies, namely $\Omega+\omega_1-\omega_2$, 2Ω, $2\Omega+\omega_1-\omega_2$, etc., – all the combinations of Ω and $\omega_1 - \omega_2$ that appear in the diverse approximations.

In order to obtain the general solution $\boldsymbol{\xi}(\boldsymbol{r}, t)$ we have to multiply the coefficients c_i by $\exp(-\mathrm{i}\omega_i t)$. We see that, beginning with the first order, the eigenvector $\boldsymbol{\xi}_1$ gets an admixture of its coupling partner, with frequency ω_2, and vice versa. The magnitude of this admixture is time-dependent, and can be considered as a contribution of a virtual state with frequency $\Omega + \omega_2$. The strength of the admixture depends on the frequency difference, the initial excitation of the oscillations and on the strength of the coupling, given by the matrix element H_{12}. The properties of the matrix elements have been discussed by Lavely & Ritzwoller (1992).

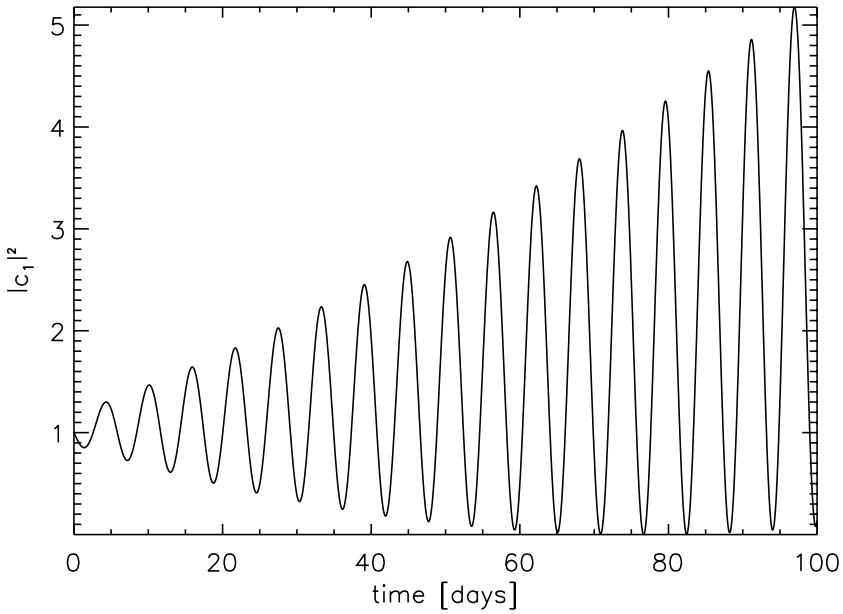

Fig. 2. Squared magnitude of the coefficient $c_1(t)$ for the coupling of two oscillations with frequencies $\nu_1 = 3000\ \mu$Hz and $\nu_2 = 3001\ \mu$Hz, respectively, and a perturbation in resonance, with $\Omega/2\pi = \nu_1 - \nu_2$, and $\varepsilon|H_{12}|/\langle H_0\rangle = 0.02$. A numerical solution of (25) and (26), with initial conditions $c_1(0) = 1$, $c_2(0) = 0$, and $\dot{c}_i = 0$, $(i = 1, 2)$.

4.2. Resonances

For certain frequencies Ω there are singular terms in the approximate solutions (20) and (23), or (29) and (30). In the first and second order of the two-coupler system this is the case for

$$\Omega = \pm(\omega_1 + \omega_2) \qquad \text{and} \qquad \Omega = \pm(\omega_1 - \omega_2)\,. \tag{31}$$

Since $|\Omega| \ll \omega_i$, the first of these cases will never happen. On the other hand, Ω and $\omega_1 - \omega_2$ may well be of similar magnitude. Hence we must discuss the second case of (31). To be specific, let us consider the case $\Omega = \omega_1 - \omega_2$. For this special case we return to the system (25) and (26).

The zero-order solution is again given by (28). In the first order we find

$$\begin{aligned} c_1^{(1)}(t) = \frac{H_{12}}{N_1}\Bigg[A_2^{(0)}\left(\frac{\mathrm{e}^{2\mathrm{i}\Omega t}-1}{4\omega_2\Omega} - \frac{\mathrm{e}^{2\mathrm{i}\omega_1 t}-1}{4\omega_1\omega_2}\right) \\ + B_2^{(0)}\left(\frac{\mathrm{e}^{2\mathrm{i}\omega_1 t}-1}{4\omega_1^2} - \frac{\mathrm{i}t\,\mathrm{e}^{2\mathrm{i}\omega_1 t}}{2\omega_1}\right)\Bigg], \\ c_2^{(1)}(t) = \frac{H_{21}}{N_2}\Bigg[A_1^{(0)}\left(\frac{\mathrm{i}t}{2\omega_2} - \frac{\mathrm{e}^{2\mathrm{i}\omega_2 t}-1}{4\omega_2^2}\right) \\ + B_1^{(0)}\left(\frac{\mathrm{e}^{2\mathrm{i}\omega_2 t}-1}{4\omega_2\Omega} - \frac{\mathrm{e}^{2\mathrm{i}\omega_1 t}-1}{4\omega_1\Omega}\right)\Bigg]. \end{aligned} \tag{32}$$

In the second order we have

$$\begin{aligned} c_1^{(2)}(t) = \frac{H_{12}H_{21}}{N_1N_2}\Bigg\{A_1^{(0)}\Bigg[\frac{(2\Omega-\omega_2)(\mathrm{e}^{2\mathrm{i}\Omega t}-1)}{16\omega_2^3\Omega^2} \\ - \frac{(2\omega_1+\omega_2)(\mathrm{e}^{2\mathrm{i}\omega_1 t}-1)}{16\omega_1^2\omega_2^3} + \frac{\mathrm{i}t}{8\omega_2^2}\left(\frac{\mathrm{e}^{2\mathrm{i}\Omega t}}{\Omega} + \frac{\mathrm{e}^{2\mathrm{i}\omega_1 t}}{\omega_1}\right)\Bigg] \\ + B_1^{(0)}\Bigg[\frac{\mathrm{e}^{2\mathrm{i}(\omega_1+\Omega)t}-1}{16\omega_1\Omega^2(\omega_1+\Omega)} \\ - \frac{\mathrm{e}^{2\mathrm{i}\omega_1 t}-1}{16\omega_1^2\Omega^2} + \frac{\mathrm{e}^{2\mathrm{i}\omega_1 t}-\mathrm{e}^{2\mathrm{i}\Omega t}}{16\omega_1\omega_2^2\Omega} - \frac{\mathrm{i}t\,\mathrm{e}^{2\mathrm{i}\omega_1 t}}{8\omega_1\omega_2\Omega}\Bigg]\Bigg\}, \end{aligned} \tag{33}$$

$$\begin{aligned} c_2^{(2)}(t) = \frac{H_{12}H_{21}}{N_1N_2}\Bigg\{A_2^{(0)}\Bigg[\frac{\mathrm{e}^{2\mathrm{i}\Omega t}-1}{16\omega_2\Omega^2(\omega_2-\Omega)} \\ + \frac{\mathrm{e}^{2\mathrm{i}\omega_1 t}-1}{16\omega_1^2\omega_2\Omega} - \frac{\mathrm{e}^{2\mathrm{i}\omega_2 t}-1}{16\omega_2^2\Omega(\omega_2-\Omega)} - \frac{\mathrm{i}t}{8\omega_1\omega_2\Omega}\Bigg] \\ + B_2^{(0)}\Bigg[\frac{\mathrm{e}^{2\mathrm{i}\omega_2 t}-1}{16\omega_2^2\Omega^2} - \frac{(\omega_1+2\Omega)(\mathrm{e}^{2\mathrm{i}\omega_1 t}-1)}{16\omega_1^3\Omega^2} \\ + \frac{\mathrm{i}t\,\mathrm{e}^{2\mathrm{i}\omega_1 t}}{8\omega_1^2\Omega} - \frac{\mathrm{i}t}{8\omega_1^2\omega_2}\Bigg]\Bigg\}. \end{aligned} \tag{34}$$

This is a resonance case. The expressions (32)–(34) contain terms with time dependencies $\propto t$. For large t these terms grow beyond any limit. The resonance frequency is the beat frequency, $\omega_1 - \omega_2$, of the two involved modes.

In contrast to the non-resonant case discussed earlier, we have included into the approximate solutions (32)–(34) all the

terms required to satisfy the initial conditions in the first and second order, namely $c_i^{(j)} = \dot{c}_i^{(j)} = 0$ for $i = 1, 2$ and $j = 1, 2$. Those terms can cause growing terms in subsequent higher orders. Thus, only the four integration constants $A_1^{(0)}, \ldots, B_2^{(0)}$ that arise in the zero-order solution are left open.

In Fig. 2 we show the behavior of the coefficient $c_1(t)$ for an example resonance case, as obtained from the numerical solution of (25) and (26). It clearly shows the linear growth with time of the oscillation amplitude, which was found in the approximate solutions. The other coefficient, $c_2(t)$, also grows beyond limits. The simultaneous growth in amplitude of both oscillations is possible because the perturbation $H_1(\boldsymbol{r}, t)$ is not Hermitian, and hence the oscillation energy is not conserved.

Of course, the growth will be limited at some stage. We suppose that this limitation is not achieved by one of the two classical mechanisms that counteract resonance, namely damping and non-linearity. Damping is very weak in the solar interior, and only in the atmosphere it might have a small effect; it is well-known that adiabatic theory reproduces the solar eigenfrequencies with a precision of 10^{-3} and better. The non-linear terms of the hydrodynamic equations could become crucial in principle. But the observed amplitudes of the solar oscillations are so small that the frequency shift that goes along with the non-linear saturation (Landau & Lifschitz 1963) does not take place. Instead, we think that the growth shown in Fig. 2 proceeds only for a limited amount of time because the coupling velocity changes. The assumption (6) of a purely periodic coupling is too crude. The initial growth time of our resonances is of order Ω^{-1}, as can be seen from the approximate solutions (32)–(34) as well as from Fig. 2; during this time the coupling velocity in the solar convection zone might change, so that the mutual growth and decay of eigenoscillations is a transitory phenomenon. Indeed, Roth (2001) found some evidence for the exchange of oscillatory power among the Sun's oscillations.

For stars other than the Sun, with different excitation mechanisms, the non-linear saturation might be crucial (Christy 1964). In addition, the superposition of several resonances may lead to chaotic behavior, and to irregular stellar variability (Perdang 1985). For the Sun we do not expect such effects.

5. Power spectra

We shall now discuss the possible consequences of a time-dependent large-scale flow to the interpretation of an observed power spectrum of solar oscillations.

The coupling of the oscillations depends on the variation of the flow field, which in the present paper is represented by the frequency Ω and the coupling matrix H_{nm}. As a result of the coupling the oscillations are mixtures of eigenstates of the unperturbed system. Thus, it is generally not possible to measure pure states. However, as long as the coupling is weak, a mixed state still consists predominantly of one of the original eigenstates, with a small admixture of other states.

In addition to the coupling, we must realize that in general the oscillations are damped, and hence the peaks in the power spectrum have a natural line width. This is true for pure as well as for mixed states. Usually the mode frequencies are determined from the observed data by fitting Lorentzians to the peaks in the power spectrum.

Our results suggest that the power of a state with frequency ν leaks into the admixed states, but also that some of the power in the admixed states originates from leakage of other states (those that couple). That means that side lobes emerge with heights that depend on the strength of the coupling and on the initial conditions. We conclude from the iterative method that these side lobes are located at $\nu \pm \Omega/2\pi$, $\nu + (\nu - \nu_n)$, $\nu + (\nu - \nu_n) \pm \Omega/2\pi$, $\nu \pm 2\Omega/2\pi$, $\nu + (\nu - \nu_n) \pm 2\Omega/2\pi$, etc., where ν_n is the frequency of a coupling partner.

For a mode with frequency $\nu = 3005.3\ \mu$Hz and $l = 22$, $n = 14$, $m = 16$, Fig. 3 displays the power distribution according to the expansion (27). The coupling partner has a frequency $\nu = 3011.1\ \mu$Hz, and $l' = 27$, $n' = 13$, $m' = 21$. For this calculation we assumed that, due to the natural damping, the single peaks can be represented by Lorentzians. Side lobes to the primary peak appear at frequencies where the diverse denominators of expressions (20) and (23) become small (notice that this example is not a resonant case). The 6 panels illustrate how the diverse side lobes contribute. We have truncated the expansion after the second order. The error of the expansion is therefore of the order $O(\varepsilon^3)$. The flow chosen for this example has a parabolic depth dependence of $u_s^t(r)$ according to Eq. (6), and $u_{\max} = 100\ \mathrm{m\,s^{-1}}$; the harmonic degree and azimuthal order are $s = t = 5$, the time dependence is $\Re[1 - \exp(\mathrm{i}\Omega t)]$. In this case the first side lobes are already about 100 times smaller than the main peak.

Due to the asymmetry of the admixture emerging from the coupling partners the center of gravity of the peak is shifted. Hence there is an effective frequency shift relative to the frequency of a mode of the equilibrium model. This means that the considerations concerning the frequency shifts that we had made for a steady-state flow, must be generalized. Time-dependent flow fields lead to diminished, asymmetric, and broadened and effectively shifted peaks in the power spectrum. The frequency shift is equivalent to an average effect of the flow. As in the case of a steady flow we find that the shift of the frequency of one mode is accompanied by a frequency shift of its coupling partner with the same magnitude, but with opposite sign. This means that, of two coupling modes with frequencies ν_1 and ν_2, one mode has side lobes at $\nu_1 + (\nu_1 - \nu_2) \pm \mathbb{N}\Omega$, the other at $\nu_2 + (\nu_2 - \nu_1) \pm \mathbb{N}\Omega$ (cf. Fig. 4). The power spectra of the two modes are mirror images of each other with respect to $(\nu_1 + \nu_2)/2$. Therefore the center of gravity of one mode is shifted in one direction, whereas the center of gravity of the other mode is shifted by the same amount into the other direction.

As for the interpretation of an observed power spectrum, we may conclude that a peak consists of a prominent main peak and several side lobes. As an example, Fig. 5 compares the result shown in Fig. 3 (lower right panel) with the power spectrum of the same mode ($l = 22$, $n = 14$, $m = 16$), as derived from MDI data. We may interpret the multitude of side lobes as a superposition of the effects of all possible couplings caused by the existent flow components in the solar convection zone. As some power is transferred from the primary peaks into the side lobes, the result is a decrease in height and

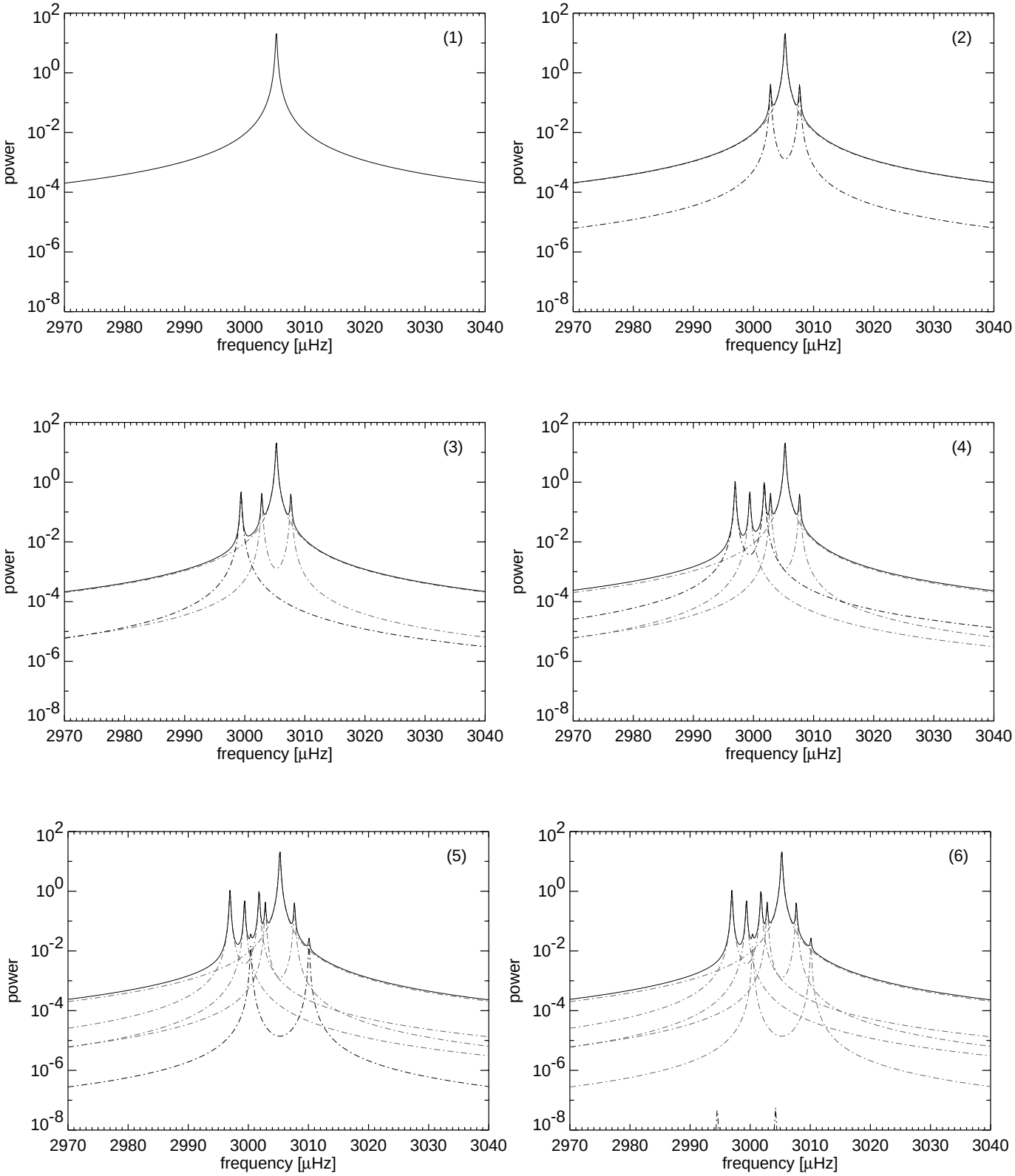

Fig. 3. Power spectrum (upper *solid* curve) of a solar p-mode with frequency $\nu_1 = 3005.3\,\mu$Hz, calculated for a perturbation by a time-dependent flow, with contributions up to order ε^2. The frequency of the coupling partner (not shown) is $\nu_2 = 3011.1\,\mu$Hz; the flow parameters are $u_{\max} = 100$ m/s, $s = t = 5$ and $\Omega/2\pi = 2.42 \times 10^{-6}\,\mathrm{s}^{-1}$. **(1)**: Unperturbed p-mode. **(2)**: p-mode with side lobes at $\nu \pm \Omega/2\pi$. **(3)**: Additional side lobe at $\nu_1 + \Delta_{12}$, where $\Delta_{12} = (\nu_1 - \nu_2)$. **(4)**: Additional side lobes at $\nu_1 + \Delta_{12} \pm \Omega/2\pi$. **(5)**: Additional side lobes at $\nu_1 \pm 2\Omega/2\pi$. **(6)**: Additional side lobes at $\nu_1 + \Delta_{12} \pm 2\Omega/2\pi$ (very small, at bottom). In addition to the sum, each panel shows the actually added power (lower *dash-dotted black* curve), and the power added in the preceding panels (*dash-dotted grey*).

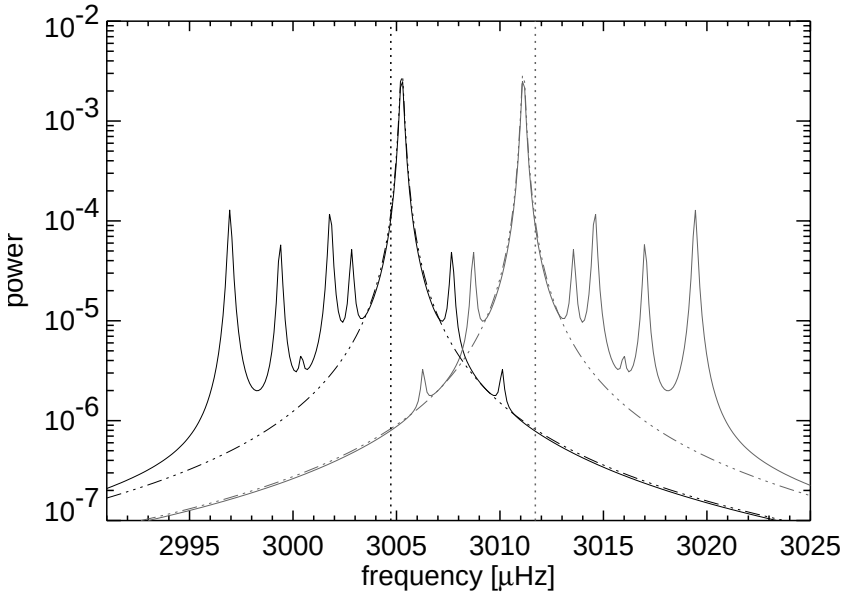

Fig. 4. Power spectra of two modes, at $\nu_1 = 3005.3\,\mu$Hz (black) and $\nu_2 = 3011.1\,\mu$Hz (grey), under time-dependent coupling by a flow field with $\Omega/2\pi = 2.42 \times 10^{-6}\,\mathrm{s}^{-1}$, $u_{\max} = 100\,$m/s, and initial conditions $A_1^{(0)} = A_2^{(0)} = 1$ and $B_1^{(0)} = B_2^{(0)} = 0$. The *dash-dotted* curves are the Lorentzian profiles of the two coupling modes, the vertical *dotted* lines mark the centers of gravity of the two resulting spectra.

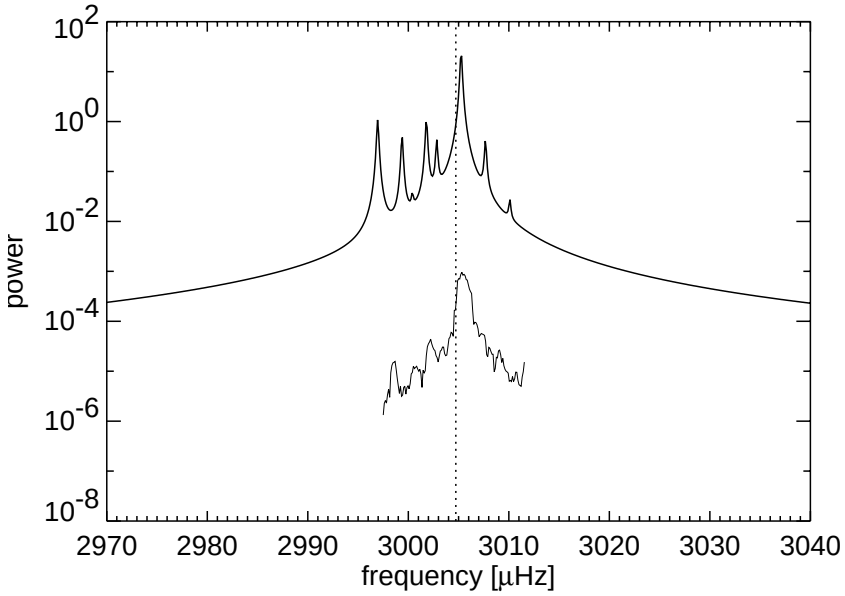

Fig. 5. Comparison of the perturbation calculation, truncated after the second order, for the *p* mode shown in Fig. 3 (*upper curve*), and a power spectrum for the same *p* mode as derived from MDI data (*lower curve*). The *dotted* line marks the center of gravity of the upper spectrum.

a broadening of the peaks. Moreover, since the distribution of side lobes is asymmetric for each of the coupling partners, there is a contribution to the peak asymmetry, which may imply an (albeit small) effective shift.

References

Christy, R. F. 1964, Rev. Mod. Phys., 36, 555
Landau, L. D., & Lifschitz, E. M. 1963, Mechanik (Berlin: Akademie-Verlag)
Lavely, E. M., & Ritzwoller, M. H. 1992, Phil. Trans. R. Soc. Lond. A, 339, 431
Perdang, J. M. 1985, in Chaos in Astrophysics, ed. J. R. Buchler, J. M. Perdang, & E. A. Spiegel, NATO ASI Ser. C, 161, 11
Roth, M., & Stix, M. 1999, A&A, 351, 1133
Roth, M., & Stix, M. 2001, ESA-SP 464, 243
Roth, M. 2001, ApJ., 559, 1165
Roth, M., Howe, R., & Komm, R. 2002, A&A, 396, 243
Stix, M. 2002, The Sun, 2nd ed. (Berlin Heidelberg: Springer)
Walter, W. 1993, Gewöhnliche Differentialgleichungen, 5. Auflage (Berlin, Heidelberg: Springer)